

## FULL PAPER

# About the enhancement of chemical yield during the atmospheric plasma synthesis of ammonia in a ferroelectric packed bed reactor

Ana Gómez-Ramírez<sup>1,2\*</sup> | Antonio M. Montoro-Damas<sup>1</sup> | José Cotrino<sup>1,2</sup> |  
Richard M. Lambert<sup>1,3</sup> | Agustín R. González-Elipe<sup>1\*</sup>

<sup>1</sup>Laboratory of Nanotechnology on Surfaces, Instituto de Ciencia de los Materiales de Sevilla (CSIC-Universidad de Sevilla), Avda. Américo Vespucio 49, 41092 Sevilla, Spain

<sup>2</sup>Facultad de Física, Departamento de Física Atómica, Molecular y Nuclear, Universidad de Sevilla, Avda. Reina Mercedes, 42022 Sevilla, Spain

<sup>3</sup>Department of Chemistry, Cambridge University, Cambridge CB2 1EW, UK

## \*Correspondence

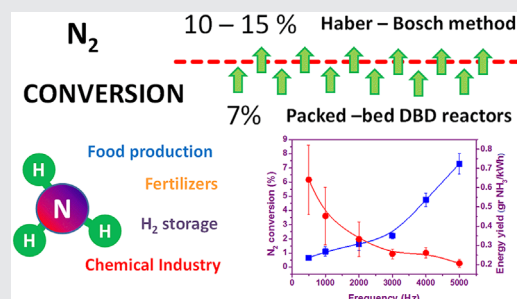
Ana Gómez-Ramírez and Agustín R. González-Elipe, Laboratory of Nanotechnology on Surfaces, Instituto de Ciencia de los Materiales de Sevilla (CSIC-Universidad de Sevilla), Avda. Américo Vespucio 49, 41092 Sevilla, Spain.

Email: anamaria.gomez@icmse.csic.es (A.G.R.); arge@icmse.csic.es (A.R.G.E.)

## Funding Information

This work was supported by Junta de Andalucía through the project P12-2265MO and from the MINECO-CSIC through the EU regional fund project RECUPERA 2020.

Plasma reactions offer an attractive alternative route for the synthesis of a variety of valuable chemical compounds. Here we investigate the parameters that determine the efficiency of ammonia synthesis in a ferroelectric packed bed dielectric barrier discharge (DBD) reactor. The effects of varying the operating frequency, the size of the ferroelectric pellets and the inter-electrode distance have been systematically studied. Under optimised conditions nitrogen conversions in excess of 7% were achieved, higher than those previously obtained using DBD reactors. These findings are discussed with respect to variations in the electrical characteristics of the reactor under operating conditions and in the light of emission spectra obtained as a function of reactant flow rates. These encouraging results signpost future developments that could very substantially improve the efficiency of ammonia synthesis by means of DBD technology.



## KEYWORDS

ammonia, dielectric barrier discharges (DBD), ferroelectric PZT pellets, nitrogen conversion, packed-bed reactor

## 1 | INTRODUCTION

Plasma excitation of nitrogen/hydrogen mixtures results in a significant degree of ammonia synthesis, reactant conversions of up to 3% having been achieved.<sup>[1-6]</sup> However, such yields and the associated low energy efficiencies do not compete with the conventional catalytic synthesis of ammonia by means of the Haber-Bosch process, where conversions of up to 10% and much higher energy efficiencies are attained.<sup>[7-9]</sup> Therefore, to enable plasma synthesis of ammonia as a potential industrial process, it is essential to

significantly improve both the conversion and the energy efficiency of current plasma processes.

Different kinds of plasma processes, encompassing low pressure microwave discharges,<sup>[2-4]</sup> gliding arc<sup>[5]</sup> or microdischarges<sup>[6]</sup> have been essayed for the synthesis of ammonia from N<sub>2</sub> and H<sub>2</sub> mixtures. Ammonia synthesis has been also achieved with the so-called dielectric barrier discharge (DBD) technique, a versatile atmospheric pressure plasma process that has been extensively used for a large variety of chemical applications.<sup>[10-14]</sup> Very recently, using a packed bed parallel plate DBD plasma reactor incorporating pellets

of a ferroelectric material to moderate the discharge, we achieved a nitrogen conversion of 2.7% employing a mixture of nitrogen and hydrogen only, without any added inert gas: to our knowledge this greatly exceeds anything reported in comparable studies.<sup>[15]</sup> It was found that the presence of a ferroelectric material, either BaTiO<sub>3</sub> or PZT, enhanced the reactor performance, an effect that we attributed both to the effect of the ferroelectric material on the discharge and to the occurrence of catalytic reactions taking place on the surface of the ferroelectric pellets. Even so, a conversion of 2.7% is far from the values that are required to make plasma technology competitive with current industrial practice.

In the present work, we investigated systematically and in detail the influence on reactor performance of the frequency of the sinusoidal applied voltage, the size of the ferroelectric pellets and the effect of the distance between electrodes. Others have studied the influence of voltage, frequency and the size of dielectric pellets on various reactions under DBD conditions.<sup>[16–20]</sup> However, the interaction between these process variables, the use of ferroelectric pellets and the inter-electrode distance has not been examined, probably because in the most commonly used cylindrical reactors with fixed-geometry, the latter cannot be adjusted.<sup>[10,20]</sup> Here, we report the effect of key experimental parameters, including the inter-electrode separation, on the properties of N<sub>2</sub>/H<sub>2</sub> mixtures and the consequences for ammonia synthesis performance, using a ferroelectrically moderated DBD reactor. Nitrogen conversions in excess of 7% were achieved, and it was shown that this value could be increased by appropriate alteration of discharge operating conditions and reactor design. These conclusions were arrived at by analysis of the electrical working parameters of the reactor and of the plasma emission spectra, along with simulation of the electrical field at the ‘necks’ between ferroelectric pellets. The simulation was done using COMSOL Multiphysics software,<sup>[21]</sup> and by the evaluation of the electron energy and density by numerical methods based on solution of the Boltzmann equation for weakly ionised gases under uniform electric fields.<sup>[22]</sup> Although conclusions were reached for the particular case of ammonia synthesis, they are of general applicability and should enable the optimisation of DBD reactor design and operating conditions for other types of reactions.

## 2 | EXPERIMENTAL SECTION

Figure 1 shows a scheme of the reactor design used in the present work, similar to that utilised by us in previous studies.<sup>[15,23]</sup> It consisted of a stainless steel chamber and a stainless steel plate as active electrode (7.5 cm in diameter) with the bottom wall of the reactor as grounded electrode. Gas feed was via a hole in the bottom wall that was covered with a

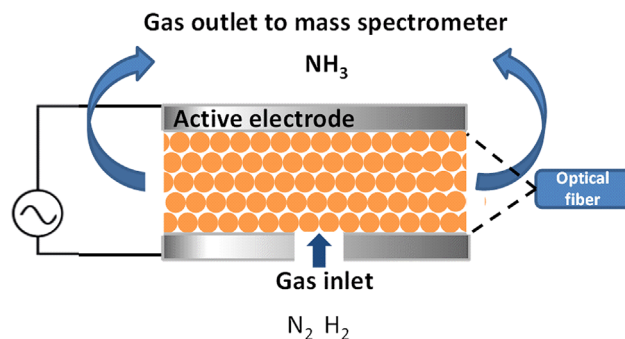


FIGURE 1 Scheme of the reactor set-up

metallic mesh to ensure electrical continuity. The adjustable inter-electrode space was filled with small spherical pellets of PZT (lead zirconate titanate), a ferroelectric material previously shown by us to maximise the efficiency of NH<sub>3</sub> synthesis.<sup>[15]</sup> The effect of varying the diameter of the ferroelectric pellets was investigated: they were prepared from PZT powders (APC International, LTD) using an intensive mixer (Eirich GmbH, RV02). After introducing the powder into the mixer, a solution 10% of PVA in water was sprayed into it until the increase in weight was 17%. This initiated the sintering process and promoted growth of pellets whose size was controlled by the strength of the mixing and shaking action. They were then maintained at 100 °C for 24 h followed by sintering in air at 835 °C for 2 h. Subsequently, to eliminate surface imperfections, the pellets were ball milled for 1 h and sized by sieving through calibrated meshes. Pellets with sizes between 0.5 and 2 mm and between 2 and 3 mm were used in the present work.

Experiments were carried out when the reactor walls had reached a temperature of 60 °C, maintained constant by thermostatic fan cooling. The extent of cooling required varied from case to case because the degree of Joule heating depended on the operating frequency of the plasma. Light emitted by the plasma discharge was collected through an optical fibre as shown in Figure 1 and analysed by optical emission spectra recorded with a monochromator Jobin-Yvon FHR640 using a diffraction grating blazed at 330 nm. Entrance and exit slit apertures were fixed at 300 μm, the integration time was 1 s and resolution was set at 0.2 nm. Spectra were collected for different discharge frequencies of the applied voltage and with a 10 mm inter-electrode space (spectral observations with smaller electrode separations were not possible due to optical limitations).

The plasma was driven by a high voltage power supply (Trek, Model PD05034) connected to a function generator (Stanford Research System, Model DS345) that provided the required waveform. The operating frequency was varied between 500 and 5000 Hz with applied voltages between 2.5 ± 0.3 and 5.5 ± 0.3 kV. A Tektronix TDS2001C oscilloscope was used to acquire the  $I(t)$  and  $V(t)$  signals by means of

a high voltage probe (attenuation factor: 1:1000) and a current probe (coil with a conversion factor of  $0.05 \text{ V mA}^{-1}$ ). The power applied to the plasma was determined from the area of the Lissajous diagrams.<sup>[24]</sup> This allowed calculation of the energy efficiency of the process, defined as ammonia production per unit of consumed energy ( $\text{g} \cdot \text{kWh}^{-1}$ ). The extent of ammonia production is given in terms of the percentage of nitrogen converted, quoted as  $\text{N}_2$  (%), i.e. percentage of nitrogen molecules converted into ammonia. It can be estimated from the flow rates of  $\text{N}_2$  reactant and  $\text{NH}_3$  product according to

$$Y_{\text{N}_2} = 100\dot{M}_{\text{NH}_3}/2\dot{M}_{\text{N}_2}.$$

where  $\dot{M}$  refers to the mass flow of these two gases.

Plasma electron mobility ( $\mu_e$ ) and energy ( $v_e$ ) were obtained with the Bolsig + Electron Boltzmann equation solver,<sup>[22]</sup> using as input parameters the gas mixture composition and the reduced electric field,  $E_0/N$ ,  $N$  being the gas density expressed as the number of molecules per unit volume and  $E_0$  the electric field calculated as described below. Electron density ( $n_e$ ) was then deduced assuming that in high pressure discharges this quantity is equal to the ratio between the current density ( $J$ ) and the product of the macroscopic electric field ( $E_0$ ), electron charge  $e$ , and electron mobility  $\mu_e$ . In accord with ref.,<sup>[25]</sup> current density,  $J$ , was calculated by assuming that the PZT pellets formed a hexagonal close packing (hcp) structure for which  $J = I/(A \cdot \alpha)$ , where  $A$  is the electrode area and  $\alpha = 0.09$  the void fraction in cross-sectional area.  $E_0$  was estimated as the ratio between the voltage drop in the inter-pellet region,  $V_{p-p}$ , and the maximum inter-pellet distance,  $d_{\text{max}}$ . This latter, taken as the free-distance left by the pellets divided by the number of holes along a pellet column (i.e., the number of pellets plus one), is estimated on the basis that the inter-electrode space is filled with an integer number of pellets. Assuming that the voltage drop is uniformly distributed along a pellet row,  $V_{p-p}$  is calculated as the ratio between the applied voltage and the number of gaps in a pellet column. Clearly, this calculation underestimates the actual value of the electrical field, particularly at the necks between pellets where plasma intensity would be enhanced.<sup>[26]</sup> The electric field distribution in the absence of plasma was simulated by means of COMSOL Multiphysics software,<sup>[21]</sup> and calculations were carried out for different PZT pellet sizes, taken as spheres, at constant inter-electrode separation (10 mm).

The reactor was fed with a stoichiometric 1:3  $\text{N}_2$ : $\text{H}_2$  mixture at a total flow rate that varied from 5.7 to 76.7 sccm. Assuming that the pellets formed a hcp structure, these flow rates correspond to gas residence times within the plasma region ranging from 121 to 9 s. In most experiments, when not otherwise stated, the flow was maintained constant at a value of  $11.5 \text{ cm}^3 \cdot \text{min}^{-1}$  (residence time 60 s). The 1:3 reactant ratio was chosen because it was found to

yield the highest conversions in our earlier study.<sup>[15]</sup> Reactant flows were delivered by calibrated mass flow controllers and the outlet gases were analysed with a mass spectrometer as described previously.<sup>[15]</sup> Repeated measurements showed that the error bar was of the order of 10% in all cases.

## 3 | RESULTS AND DISCUSSION

### 3.1 | Effect of operating frequency

In a first series of experiments, the frequency of the applied voltage varied between 500 and 5000 Hz for two reactor configurations characterised by inter-electrode separations of 3 and 10 mm with the same pellet size of 0.5–2 mm. Plasma ignition voltages for these two inter-electrode gaps were  $2.5 \pm 0.3$  and  $5.5 \pm 0.3$  kV, respectively. These voltages gave the highest efficiencies in our earlier work, where the effect of applied voltage was studied.<sup>[15]</sup> As is apparent from Figure 2a and b, conversion increased almost linearly up to

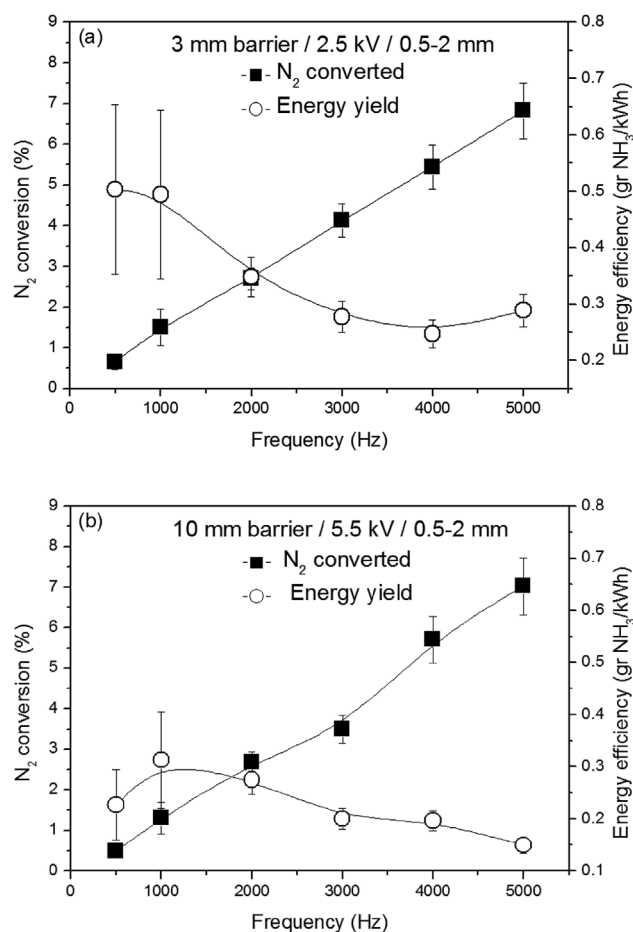


**FIGURE 2**  $\text{N}_2$  conversion and energy efficiency as a function of operating frequency. Electrode gaps were 3 (top) and 10 mm (bottom) and the applied voltages were  $2.5 \pm 0.3$  and  $5.5 \pm 0.3$  kV, respectively. Pellet size range was 0.5–2 mm

a maximum achievable value of ca. 7% for both conditions. The energy efficiency was higher with the smaller gap, although in both cases there was an overall decrease with operating frequency. The maximum achievable  $N_2$  conversion of 7% at 5000 Hz very substantially exceeds the maximum achievable value of 2.7% previously obtained at 6 kV and 500 Hz. To our knowledge, this conversion yield surpasses those previously achieved by others,<sup>[11,12]</sup> and specifically those reported by Bai et al. (1.25%),<sup>[14]</sup> Hong et al. (4.2%, using Ar as carrier gas),<sup>[13]</sup> Peng et al. (approximately 4%)<sup>[27]</sup> and Hong et al. (2%),<sup>[10]</sup> which correspond to the highest previously reported values.

Experiments were also carried out with 3 mm pellets, an inter-electrode space of 10 mm and applied voltages of  $4.1 \pm 0.3$  and  $5.5 \pm 0.3$  kV. Varying the frequency under these operating conditions gave the conversions and energy efficiencies shown in Figure 3. For both voltages, conversion increased with frequency: at  $4.1 \pm 0.3$  kV the effect was very pronounced for frequencies above 2000 Hz. In common with the results illustrated in Figure 2, increased conversion correlated with decreased energy efficiency. It is especially noteworthy that in this case increasing the operating voltage to 5.5 kV produced a huge enhancement in conversion with frequency to 7.2% at 2000 Hz. Observations at higher frequencies with this pellet size were not possible because electrical arcing between the two electrodes prevented attainment of stable discharges. This is a highly promising finding that provides a signpost for future investigations: it should be possible to achieve even higher conversions by appropriately optimising reactor architecture and operating conditions to circumvent electrical shorting. For example, addition of a thin dielectric layer on the top of ferroelectric pellet barrier could eliminate short circuits between the latter and the bare metal electrode.

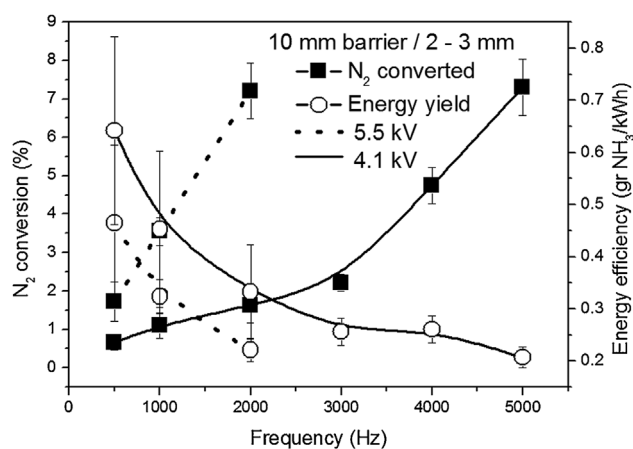


**FIGURE 3**  $N_2$  conversion and energy efficiency as a function of operating frequency for an electrode gap of 10 mm and applied voltages of  $4.1 \pm 0.3$  and  $5.5 \pm 0.3$  kV. Pellet size 2–3 mm

### 3.2 | Reactor electrical characteristics and electron densities

In order to gain insight into the effect of electrical properties on ammonia production, the electrical behaviour of the reactor under operating conditions was analysed. The  $I(t)$  and  $V(t)$  curves had similar shapes consisting of a well-defined sinusoid in the latter case and a phase shifted sinusoid with slight deformations in the former (Supporting Information S1). Lissajous curves derived from the  $V(t) - I(t)$  data are shown in Figure 4 for the different operating frequencies. With increasing frequency they evolve from an elongated to a more rounded shape. This corresponds to a progressive increase in the capacitance of the system in the absence of plasma as determined by the slope of the curve in the positive voltage branch.<sup>[28]</sup> As the geometry of the system was constant during the measurements, the increase in the capacitance (see Figure 4) must be due to changes in the dielectric constant of PZT. The effects of temperature and frequency on the dielectric properties of PZT are known.<sup>[29–35]</sup> Unlike the strong effect of temperature on the dielectric constant of PZT perovskites,<sup>[29–32,34]</sup> e.g. from 625 to 1125 at 298 and 473 K and at a constant frequency of 1 kHz,<sup>[36]</sup> frequency variation by itself causes a negligible decrease in dielectric constant.<sup>[30,33,35]</sup> Accordingly, we tentatively attribute the observed increases in capacity (c.f. Figure 4) and chemical conversion (c.f. Figures 2 and 3) with frequency to local enhancements in temperature in localised regions between pellets where the electric field and plasma would be much more intense. Such local heating with frequency is an analogous effect to the universally recognised microwave heating in a dielectric medium,<sup>[37]</sup> and would be related with the switching of ferroelectric domains during the application of the AC field.<sup>[38]</sup> Temperature increases up to

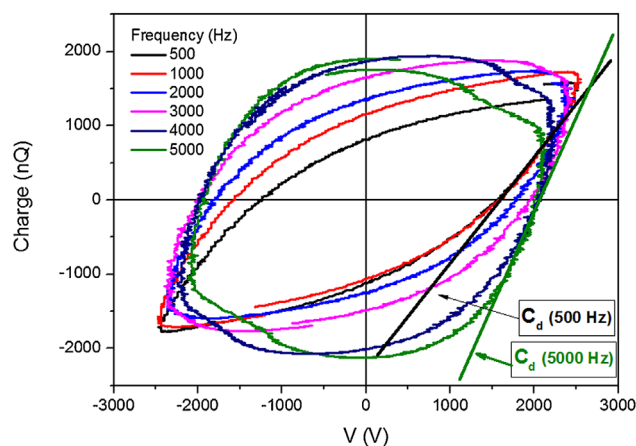


**FIGURE 4** Lissajous curves for the reactor operated at the indicated frequencies with 3 mm inter-electrode gap, 0.5–2 mm pellets and a voltage of  $2.5 \pm 0.3$  kV. The straight lines plotted in the figure are used to determine the capacitance of the system according to ref.<sup>[28]</sup>



60 °C at frequencies as low as 60 Hz have been reported for PZT ceramics.<sup>[39]</sup>

Global values of electron densities and energies were estimated for comparative purposes, as explained in Section 2. Figure 5 top panel shows the calculated values of electron density which clearly exhibits a marked increase with operating frequency. At first sight, this might account for the increase in nitrogen conversion illustrated in Figures 2 and 3. However, the increase of  $n_e$  with frequency is not sufficient to justify the observed increase of conversion data because no similar correlations appear between  $n_e$  and other variables (pellet size and inter-electrode distance) which also affect conversion (see, e.g. the bars for two pellet sizes and 10 mm inter-electrode distance in Figure 5 top).

Average electron energies estimated using the Bolsig+ code,<sup>[21]</sup> according to the procedure described in Section 2, are shown in Figure 5 (bottom panel). These calculated values are not expected to be quantitative; rather they provide an indication that can account for observed tendencies in the performance of the plasma system. According to the figure,  $v_e$

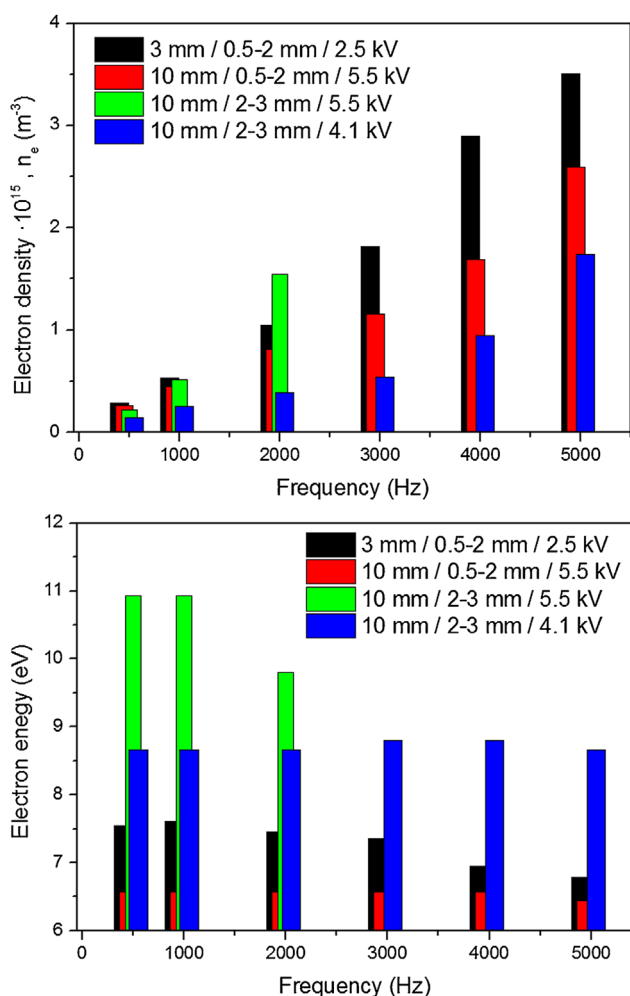


**FIGURE 5** (Top) Electron density as a function of operating frequency for the indicated working conditions. (Bottom) Idem for the average electron energy determined using the Bolsig+ code

does not vary significantly with the operating frequency, although it does vary with other parameters namely pellet size and applied voltage, reaching maximum values for 2–3 mm and 5.5 kV, respectively. We propose that conversion depends on both  $v_e$  and  $n_e$  according to a complex reaction pathway involving a number of intermediate steps.

To determine electron energies, the Bolsig+ code makes use of an average electrical field  $E_0$  which, as explained in the experimental section, has been estimated from the applied voltage incorporating corrections that take into account the filling of the inter-electrode space with ferroelectric pellets. However, as previously reported by Bogaerts et al. for the case of dielectric pellets,<sup>[26]</sup> in packed bed DBD reactors, the spatial distribution of the electric field is not homogeneous and reaches much higher values at the necks between pellets. It is expected that these inhomogeneities are even more pronounced with ferroelectric pellets because they are characterised by much higher values of dielectric constant. Using the COMSOL Multiphysics Software,<sup>[21]</sup> we simulated the electric field distribution in a model system consisting of spherical pellets beads of two different diameters. As is apparent in Figure 6, the calculated electric field distribution is maximised at the necks between pellets and is much higher for the large pellets than the smaller ones (note the different voltage scales in the figure).

Assuming a similar behaviour in the actual packed bed reactor, namely an inhomogeneous distribution of plasma density that will be higher at points where the electrical field is maximum, i.e. at the necks of the larger pellets of bigger size,<sup>[25,26,40,41]</sup> we conclude that our calculations in Figure 6 of the magnitude of electrical field function (this tightly related with the distribution of plasma density) are in good

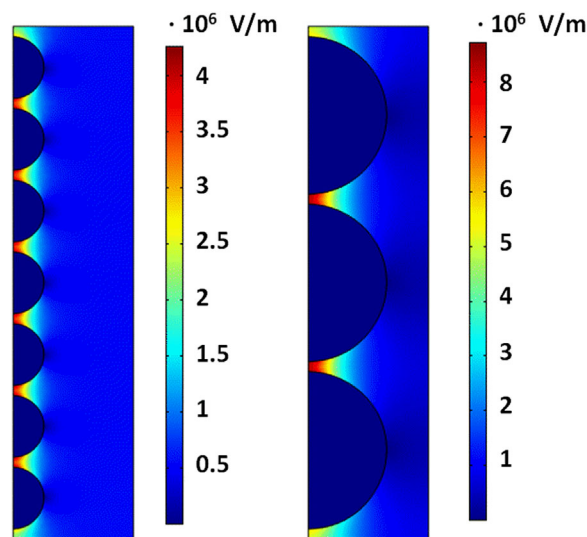


**FIGURE 6** Distribution of electric field intensity determined with the COMSOL software for two idealised ferroelectric systems formed by spherical beads of 1.25 (left) and 3.12 (right) mm. Note the different electric field scales

qualitative agreement with the  $E_0$  values used to determine the average electron energies via the Bolsig+ code as shown in Figure 5, thus providing a qualitative explanation for the observed trends in conversion illustrated in Figures 2 and 3 as a function of frequency. These calculations of local variations of electrical field also sustain the hypothesis that local increases in temperature growing with the operating frequency and pellet size could lead to substantial changes in the dielectric constant of the ferroelectric pellets and, consequently, to further enhancements in the intensity of the plasmas at these points and in the overall chemical conversion of the process.

### 3.3 | Optical emission spectra and residence time effects

The above analysis provides a qualitative account of the dependence of conversion on frequency, pellet size and inter-electrode gap. However, the relatively low energy efficiency of the process (Figures 2 and 3) remains to be explained. In earlier work on methane reforming and formaldehyde synthesis in DBD packed-bed reactors, [23,42] we showed that decreases in energy efficiency are likely due to the occurrence of back-reactions and other intermediate processes that consume a substantial amount of input energy without contributing to the formation of desired products (by ‘back reactions’ we mean any processes that contribute to decomposition of ammonia molecules, e.g.  $\text{NH}_3 + e^- \rightarrow \text{NH}^* + 2\text{H}^* + e^-$ ). To check whether similar processes were at work, in the present case we first examined the dependence of conversion rates and energy efficiency on the total flow of reactants at a fixed frequency. The total flow rates used were 5.7, 11.5, 23, 38.3 and 76.6 sccm, corresponding to residence times of 121, 60, 30, 18 and 9 s, respectively. These experiments showed (Figure 7) that conversion decreased and energy efficiency increased for lower residence times. The former suggests a reduced reaction probability due the shorter residence time of reactants in the reaction zone, while the latter indicates that at high reactant flows less energy is utilised in secondary reactions or other parasitic processes that reduce the formation of ammonia. This behaviour resembles that observed previously, [23,42] leading to the conclusion that undesired back reactions (decomposition of ammonia) are minimised at short residence times.

OES analysis of the plasma confirms this view. Figure 8 shows a spectrum taken at 5000 Hz. The overall spectral intensity increased with frequency in much the same manner that the evolution of conversion in Figures 2 and 3. The spectral lines can be assigned to various excited nitrogen species, specifically the second positive system of  $\text{N}_2$  and the first negative system of  $\text{N}_2^+$ . The first, corresponding to the transition [ $\text{C}^3\Pi \rightarrow \text{B}^3\Pi$ ], is identified by the emission line at 357.9 nm, while the line at 391.4 is due to the [ $\text{B}^2\Sigma_u^+ \rightarrow \text{X}^2\Sigma_g^+$ ] transition. Excited  $\text{NH}^*$  radicals

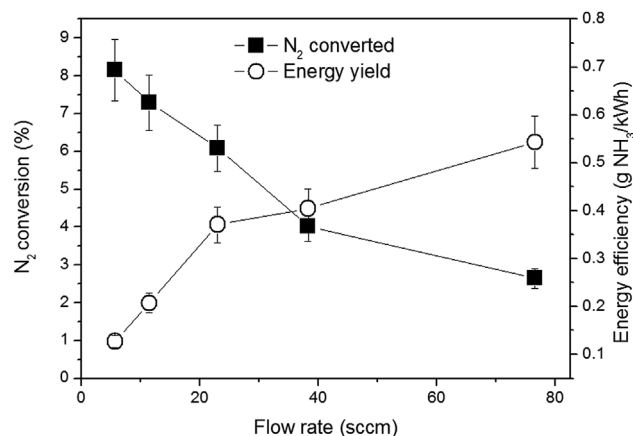


FIGURE 7 Dependence of conversion and energy efficiency on flow rate of nitrogen for an applied voltage of  $4.1 \pm 0.3$  kV with 2–3 mm ferroelectric pellets

( $\text{A}^3\Pi \rightarrow \text{X}^3\Sigma$  transition) were also observed at 336.0 and 337.0 nm, the former with a higher relative intensity. [43,44] As before, [15] no lines attributable to atomic hydrogen were observed. In our earlier study of this system, we identified  $\text{N}_2^+$  and  $\text{NH}^*$  as two signature species whose intensity

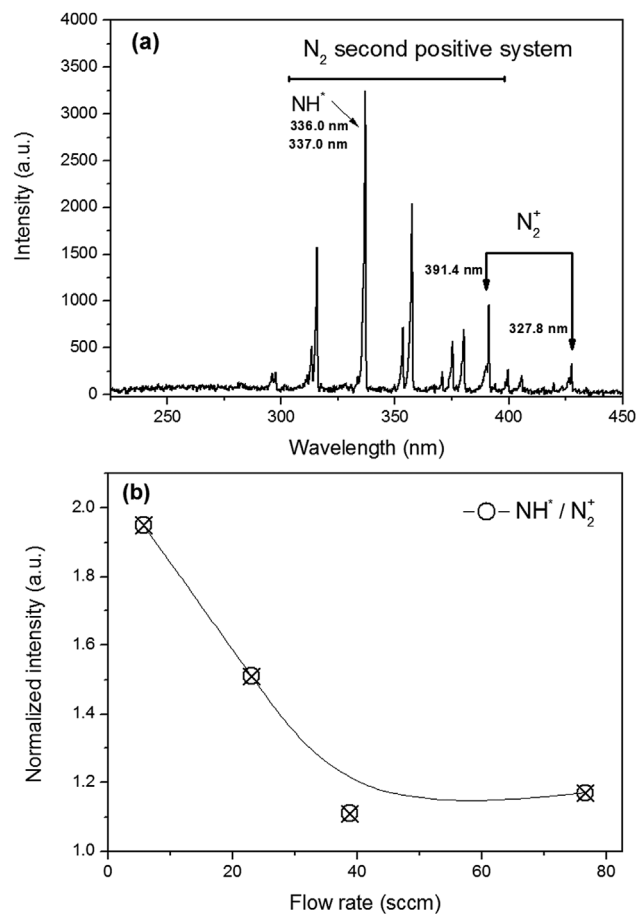


FIGURE 8 (a) Optical emission spectra recorded at  $4.1 \pm 0.3$  kV at 5000 Hz. (b) Normalised intensity to  $\text{N}_2^+$  as the residence time of the gases decreases. Inter-electrode distance 10 mm and pellet size 2–3 mm

variation as a function of voltage could indicate a possible reaction mechanism.<sup>[5,6,11–14]</sup> Specifically,  $N_2^+$ , formed by  $N_2 + e^- \rightarrow N_2^+ + 2e^-$  or  $N_2^* + N_2^* \rightarrow N_2^+ + N_2 + e^-$ , is the intermediate species involved in the formation of ammonia, while  $NH^*$  stems from both the formation and decomposition of ammonia (reactions  $N_2^+ + H_2 \rightarrow NH^*$  and  $NH_3 + e^- \rightarrow NH^* + 2H^* + e^-$ , respectively). Analysis of the relative emission intensities due to these species showed that the ratio  $NH^*/N_2^+$  decreased with gas flow (Figure 8 bottom panel). As the OE spectra were taken at fixed voltage and frequency, no changes are expected neither in the overall properties of the plasma (electron energy and density should be substantially the same) nor in the reaction mechanisms which would involve the majority  $N_2$  and  $H_2$  molecules present in a similar proportion irrespective of the total gas flow. Therefore, the observed trend of the  $NH^*/N_2^+$  intensity ratio must be attributed to decrease in the rate of formation of  $NH^*$  radicals resulting from the decomposition of minority  $NH_3$  molecules whose residence time drastically decreases when increasing the gas flow rate.

Apart from the plasma processes outlined above, it is noteworthy that surface reactions may also be involved in the formation of ammonia. For example, some of the intermediate processes leading to ammonia formation ( $N_2^+ + 2H \rightarrow NH^*$ ,  $NH + 2H \rightarrow NH_2 + H$ ,  $NH_2 + 2H \rightarrow NH_3 + H$ ) are reported to occur at plasma-exposed surfaces, such as reactor walls.<sup>[45–47]</sup> In our previous publication on ammonia production, we pointed out that ferroelectric material surfaces could be acting as a catalyst, thus promoting the reaction.<sup>[15]</sup> Although plasma-catalysis processes have been claimed to enhance the ammonia yield,<sup>[48]</sup> plasma-catalyst synergetic effects are far from being understood and deserve investigation as an important research theme in future investigations.

## 4 | CONCLUSIONS

From a mechanistic point of view, plasma synthesis of ammonia from  $N_2$  and  $H_2$  is a simple reaction that allows the derivation of principles relating mechanistic information to plasma operating conditions. In pursuit of optimising DBD reaction conditions, the present findings provide important indications about which operational parameters may be advantageously explored for application in other systems. It has been found that in ferroelectric packed bed DBD reactors frequency plays a critical role in enhancing electron density and energy and, consequently, the reaction yield. We propose that this enhancement is linked to an increase in electrical field at the necks between ferroelectric pellets. At these hot spots local increases in temperature would induce sharp increases in dielectric constant that could be responsible for the observed changes in the macroscopic capacitance of the system. The almost linear increase in conversion with

frequency would be the consequence of these changes in the intrinsic electrical properties of the reactor during plasma ignition. Another important conclusion of our work is that these electrical characteristics can be modified by adjusting working parameters such as the inter-electrode spacing and the size of the ferroelectric pellets. By varying these and the applied voltage and frequency, we were able to substantially increase all plasma variables and the nitrogen conversion rate at relatively low frequencies. Yet higher increases in performance were prevented by electrical short-circuiting through the pellet barrier.

Despite the unprecedented nitrogen conversion rates of 7% found here, the energy efficiency of the process is uncompetitive with the classical route for ammonia synthesis. The dependence of conversion on reactant flow and analysis of the plasma emission spectra strongly suggest that back-reactions and other parasitic excitation processes are responsible for the relatively low energetic efficiency. At first sight, the opposite dependences of nitrogen conversion and process energy efficiency on frequency may appear to preclude the possibility of DBD plasma chemistry achieving competitive efficiency in comparison to other methods. However, the present findings signpost possible means for simultaneously increasing both conversion and energy efficiency. Possible strategies include modifying the reactor configuration (including the architecture of barrier material), sequential injection of reactants and pulsing of the discharge. Moreover, the use of ammonia trapping and residual gas recirculation methodology could very substantially increase the limited chemical efficiency achieved by conventional single pass operation.

## ACKNOWLEDGEMENTS

We acknowledge financial support from Junta de Andalucía through the project P12–2265 MO and from the MINECO-CSIC through the EU regional fund project RECUPERA 2020.

## REFERENCES

- [1] V. Hessel, A. Anastasopoulou, Q. Wang, G. Kolb, J. Lang, *Catal. Today* **2013**, *211*, 9.
- [2] J. Nakajima, H. Sekiguchi, *Thin Solid Films* **2008**, *516*, 4446.
- [3] H. Uyama, O. Matsumoto, *Plasma Chem. Plasma Process.* **1989**, *9*, 421.
- [4] H. Uyama, O. Matsumoto, *Plasma Chem. Plasma Process.* **1989**, *9*, 13.
- [5] M. Bai, Z. Zhang, M. Bai, X. Bai, H. Gao, *Plasma Chem. Plasma Process.* **2008**, *28*, 405.
- [6] J. H. Helden, W. Wagemans, G. Yagci, R. A. B. Zijlmans, D. C. Schram, R. A. H. Engeln, G. Lombardi, G. D. Stancu, J. Röpcke, *J. Apply. Phys.* **2007**, *101*, 043305.
- [7] H.-H. Kim, Y. Teramoto, A. Ogata, H. Takagi, T. Nanba, *Plasma Chem. Plasma Process.* **2016**, *36*, 45.

- [8] J. W. Erisman, M. A. Sutton, J. Galloway, Z. Klimont, W. Winiwarter, *Nat. Geosci.* **2008**, *1*, 636.
- [9] G. Ertl, *Angew. Chem. Int. Ed.* **2008**, *47*, 3524.
- [10] J. Hong, M. Aramesh, O. Shimoni, D. H. Seo, S. Yick, A. Greig, C. Charles, S. Prawer, A. B. Murphy, *Plasma Chem. Plasma Process.* **2016**, *36*, 917.
- [11] T. Mizushima, K. Matsumoto, J. Sugoh, H. Ohkita, N. Kakuta, *Appl. Catal. A Gen.* **2004**, *265*, 53.
- [12] T. Mizushima, K. Matsumoto, H. Ohkita, N. Kakuta, *Plasma Chem. Plasma Process.* **2007**, *27*, 1.
- [13] J. Hong, S. Prawer, A. B. Murphy, *IEEE Trans. Plasma Sci.* **2014**, *42*, 2338.
- [14] M. Bai, Z. Zhang, X. Bai, M. Bai, W. Ning, *IEEE Trans. Plasma Sci.* **2003**, *31*, 1285.
- [15] A. Gómez-Ramírez, J. Cotrino, R. M. Lambert, A. R. González-Elipse, *Plasma Sources Sci. Technol.* **2015**, *24*, 065011.
- [16] T. Butterworth, R. Elder, R. Allen, *Chem. Eng. J.* **2016**, *293*, 55.
- [17] T. J. Ma, Y. Q. Xu, *Adv. Mater. Res.* **2013**, *781–784*, 1637.
- [18] R. Zhang, T. Yamamoto, D. S. Bundy, *IEEE Trans. Ind. Appl.* **1996**, *32*, 113.
- [19] D. Mei, X. Zhu, Y.-L. He, J. D. Yan, X. Tu, *Plasma Sources Sci. Technol.* **2015**, *24*, 015011.
- [20] R. Snoeckx, Y. X. Zeng, X. Tu, A. Bogaerts, *RSC Adv.* **2015**, *5*, 29799.
- [21] Available at: [www.comsol.com](http://www.comsol.com).
- [22] G. J. M. Hagelaar, L. C. Pitchford, *Plasma Sci. Sources Technol.* **2005**, *14*, 722. Available at: <http://nl.lxcat.net/solvers/BOLSIG+/>.
- [23] A. M. Montoro-Damas, J. J. Brey, M. A. Rodríguez, A. R. González-Elipse, J. Cotrino, *J. Power Sources* **2015**, *296*, 268.
- [24] T. C. Manley, *Trans. Electrochem. Soc.* **1943**, *84*, 83.
- [25] K. Takaki, J. S. Chang, K. G. Kostov, *IEEE Trans. Dielectr. Electr. Insul.* **2004**, *11*, 481.
- [26] K. V. Laer, A. Bogaerts, *Plasma Sources Sci. Technol.* **2016**, *25*, 015002.
- [27] P. Peng, Y. Li, Y. Cheng, S. Deng, P. Chen, R. Ruan, *Plasma Chem. Plasma Process.* **2016**, *36*, 1201.
- [28] A. V. Pipa, T. Hoder, J. Koskulics, M. Schmidt, R. Brandenburg, *Rev. Sci. Instrum.* **2012**, *83*, 075111.
- [29] Q. M. Zhang, H. Wang, N. Kim, L. E. Cross, *J. Appl. Phys.* **1994**, *75*, 454.
- [30] Properties of PZT-Based Piezoelectric Ceramics Between-150 and 250°C, M. W. Hooker, Nasa Report – NASA / CR- 1998-208708, **1998**.
- [31] C. Miclea, C. Tanasoiu, L. Amarande, C. F. Miclea, C. Plavitu, M. Cioangher, L. Trupina, C. T. Miclea, C. David, *Rom. J. Inf. Sci. Technol.* **2007**, *10*, 243.
- [32] T. Singh, A. Kumar, U. C. Naithani, *Indian J. Pure Appl. Phys.* **2012**, *48*, 47.
- [33] S. K. Han, S. J. Lee, J. Kim, K.-Y. Kang, *J. Korean Phys. Soc.* **1998**, *32*, S364.
- [34] *Broadband Dielectric Response in Hard and Soft PZT: Understanding Softening and Hardening Mechanisms*, L. Jin, PhD thesis, THÈSE NO 4988, École Polytechnique Fédérale De Lausanne, Lausanne, **2011**.
- [35] E. M. Bourim, H.-Y. Kim, J.-S. Yang, J.-W. Yang, K.-S. Woo, J.-H. Song, S.-K. Yun, *Sensor. Actuat. A Phys.* **2009**, *155*, 290.
- [36] *Microstructural Evolution in Lead Zirconate Titanate (PZT) Piezoelectric Ceramics*, C.-C. Chung, Doctoral Dissertations, Paper 293, University of Connecticut, Connecticut, **2014**.
- [37] *Industrial Microwave Heating* (Eds.: A.T. Johns, G. Ratcliff, J.R. Platts). Peter Peregrinus Ltd., London, UK **1993**.
- [38] O. V. Malyskhina, A. Yu, *Ferroelectrics* **2015**, *480*, 10.
- [39] H.-W. Wang, S.-Y. Cheng, *Tamkang J. Sci. Eng.* **2000**, *3*, 243.
- [40] *Modelling of a packed bed dielectric barrier discharge plasma reactor*, K. V. Laer, S. Kolev, A. Bogaerts, Book of abstracts – 22nd International Symposium on Plasma Chemistry, Antwerp, Belgium, **2015**.
- [41] K. V. Laer, A. Bogaerts, *Energy Technol.* **2015**, *3*, 1038.
- [42] A. Gómez-Ramírez, V. J. Rico, J. Cotrino, A. R. González-Elipse, R. M. Lambert, *ACS Catal.* **2014**, *4*, 402.
- [43] *The Identification of Molecular Spectra* (Eds.: R. W. B. Pearse, A. G. Gaydon), Chapman and Hall Ltd., London **1965**.
- [44] N. K. Bibinov, A. A. Fateev, K. Wiesemann, *J. Phys. D: Appl. Phys.* **2001**, *34*, 1819.
- [45] K. S. Yin, M. Venugopalan, *Plasma Chem. Plasma Process.* **1983**, *3*, 343.
- [46] H. Kiyooka, O. Matsumoto, *Plasma Chem. Plasma Process.* **1996**, *16*, 547.
- [47] O. Nomura, *Technocrat* **1983**, *16*, 29.
- [48] B. S. Patil, Q. Wang, V. Hessel, J. Lang, *Catal. Today* **2015**, *256*, 49.

#### SUPPORTING INFORMATION

Additional Supporting Information may be found online in the supporting information tab for this article.

**How to cite this article:** Gómez-Ramírez A, Montoro-Damas AM, Cotrino J, Lambert RM, González-Elipse AR. About the enhancement of chemical yield during the atmospheric plasma synthesis of ammonia in a ferroelectric packed bed reactor. *Plasma Process Polym.* 2017;14:e1600081. <https://doi.org/10.1002/ppap.201600081>